Chemical Engineering Journal 146 (2009) 237–243

Contents lists available at ScienceDirect

Chemical Engineering Journal

journal homepage: www.elsevier.com/locate/cej

Effect of synthesis conditions on nano-iron (hydr)oxide impregnated granulated activated carbon

Kiril D. Hristovski[a,*], Paul K. Westerhoff[b,1], Teresia Möller[c,2], Paul Sylvester[c,3]

[a] Environmental Technology Laboratory, Arizona State University, Polytechnic Campus, 6075 South Williams Campus Loop West, Mesa, AZ 85212, United States
[b] Department of Civil and Environmental Engineering, Arizona State University, Box 5306, Tempe, AZ 85287-5306, United States
[c] SolmeteX Inc., 50 Bearfoot Road, Northborough, MA 01532, United States

ARTICLE INFO

Article history:
Received 27 February 2008
Received in revised form 7 April 2008
Accepted 30 May 2008

Keywords:
Arsenate
Iron (hydr)oxide
Granulated activated carbon
Treatment
Water
Nanoparticle

ABSTRACT

The iron content, the distribution and morphology of iron (hydr)oxide-nanostructures, and the arsenic adsorption capacity of iron impregnated granulated activated carbon (Fe-GAC) differed depending upon the synthesis conditions used. Several Fe-GAC samples were synthesized with varying reaction contact times and reagent solution concentrations. The iron content of the Fe-GAC ranged from 0.5 to 16% Fe/g of dry media. The iron (hydr)oxide nanoparticles synthesized via the ferric/alcohol and ferrous/oxidation methods had spherical and teeth-like morphologies, respectively, based on focus ion beam/scanning electron microscope. The spherical nanoparticles had diameters between 20 and 100 nm and were distributed throughout the media, forming clusters in the pores of the Fe-GAC. In contrast, the teeth-like nanoparticles were about 30 nm long and 5 nm thick. They were distributed in the outer layers of the carbon. The arsenate affinities of the synthesized Fe-GAC samples were evaluated in batch adsorption experiments conducted in 10 mM $NaHCO_3$-buffered ultrapure water at pH values ranging from 6.2 to 10.0. In general, when evaluated under the same conditions, the Fe-GAC prepared using the oxidation step and ferrous ions had almost an order of magnitude higher arsenate adsorption capacity than the Fe-GAC produced via direct precipitation from alcohol.

1. Introduction

Arsenic, a class A human carcinogen, occurs naturally in soils and water, but it also enters the environment due to anthropogenic sources [1,2]. Many community water systems and private wells in North America and around the world contain arsenic concentrations exceeding the maximum contaminant limit (MCL) of 10 μg/L recently lowered by the US EPA, European Union (EU) and World Health Organization (WHO) [3–7]. This new regulatory pressure has increased interest in the development of new or improved technologies that economically remove arsenic from water.

Metal (hydr)oxides impregnated in granulated activated carbon (GAC) or polymeric resin beads can be used to remove arsenate or other contaminants [8–12]. Although several studies have been conducted on arsenate removal by iron-containing GAC adsorbents, limited reports address the impact of synthesis conditions on the distribution of iron (hydr)oxide nanoparticles through the modified GAC (Fe-GAC) particles. The goal of this study was to evaluate the impact of synthesis variables (i.e., iron concentration, contact time, and effect of pre-oxidation) on the iron content, the morphology and distribution of iron-containing nanostructures, and the arsenic removal capacity of Fe-GAC. Two different synthetic routes were used: (1) Fe(II) and an oxidant ($KMnO_4$), and (2) Fe(III) and direct precipitation in alcohol. The synthesized Fe-GAC adsorbent materials were characterized by elemental analysis, electron dispersion X-ray (EDX) microanalysis, surface charge analysis, and focused ion beam/scanning electron microscopy (FIB/SEM) techniques. The role of manganese in the Fe(II)/$KMnO_4$ synthesis was tracked via mass balance calculations. The capacities of the Fe-GAC samples to remove arsenic were determined by estimating Freundlich adsorption isotherm parameters in bicarbonate solution using the batch method.

* Corresponding author. Tel.: +1 480 727 1291; fax: +1 480 727 1684.
E-mail addresses: kiril.hristovski@asu.edu (K.D. Hristovski), p.westerhoff@asu.edu (P.K. Westerhoff), tmoller@solmetex.com (T. Möller), psylvester@solmetex.com (P. Sylvester).
[1] Tel.: +1 480 965 2885; fax: +1 480 965 0557.
[2] Tel.: +1 508 393 5115; fax: +1 508 393 1795.
[3] Tel.: +1 508 393 5115; fax: +1 508 393 1795.

1385-8947/$ – see front matter © 2008 Elsevier B.V. All rights reserved.
doi:10.1016/j.cej.2008.05.040

Table 1
Synthesis conditions and iron content of the Fe-GAC media synthesized via the Fe(III)/alcohol method

Fe-GAC ID	Fe^{3+} concentration in alcohol	Contact time of GAC and solution (min)	%Fe in dry Fe-GAC
M1	0.03N	15	0.5
M2	0.03N	45	0.5
M3	0.03N	180	0.5
M4	0.3N	15	3.3
M5	0.3N	45	2.2
M6	0.3N	180	2.2
M7	3N	15	9.1
M8	3N	45	9.0
M9	3N	180	9.2
M10	6N	15	12.4
M11	6N	45	12.5
M12	6N	180	11.4
Control	NA	NA	<0.05

2. Experimental approach

2.1. Preparation of the iron-modified granulated activated carbon (Fe-GAC)

Lignite-based GAC (HD-3000, US mesh 8 × 30, NORIT Americas Inc., USA) was impregnated with iron (hydr)oxide using two different synthesis methods. HD-3000 GAC was selected as the base support material because of its macroporous structure, large pore volume, and the low cost of lignite coal [13].

In the first method, GAC is pretreated with $KMnO_4$ and then brought in contact with a Fe(II)/water solution to form ferric (hydr)oxide nanoparticles [14]. Specifically, 50 g of air-dried GAC was mixed with 500 mL $KMnO_4$ solution in amber glass/teflon cap 1 L bottles at 30 rpm under the conditions reported in Table 1. This pretreated GAC was decanted and rinsed repeatedly with ultrapure water (<1 μS/cm) until no purple/pink color (from the permanganate solution) was observed. The repeated rinse facilitated cooling of the media to room temperature (20 ± 2 °C) which was increased as a result of heat generated during the pretreatment process. The pretreated GAC was subsequently mixed with a 1-M solution of $FeSO_4{\cdot}7H_2O$ for 6 h to oxidize the Fe(II) and precipitate the iron (hydr)oxide nanoparticles. During the Fe(II) oxidation step, the generation of H^+ results in a decrease in pH. This is illustrated by Eq. (1), in which Mn^{4+} is reduced to Mn^{2+}:

$$2Fe^{2+} + MnO_{2(s)} + 2H_2O \rightarrow 2FeOOH_{(s)} + Mn^{2+} + 2H^+, \quad \Delta E^{\circ}_{Mn(IV)\rightarrow Mn(II)} = 0.453$$

The formula $FeOOH_{(s)}$ indicates the formation of an amorphous ferric (hydr)oxide precipitate. To remove the excess protons and non-GAC bound iron (hydr)oxide precipitate, the synthesized Fe-GAC was repeatedly rinsed, soaked overnight in a solution of 1% $NaHCO_3$, and stored wet.

In the second method, Fe(III) is precipitated as iron (hydr)oxide nanoparticles using a modified form of a proprietary synthetic process developed by SolmeteX [15]. In this synthesis, 50 g of air-dried GAC (US mesh size 8 × 30) was mixed with 500 mL of Fe(III)/alcohol solution according to the concentrations and contact times given in Table 2. The iron impregnated GAC was filtered and then combined with a 7.5% NaOH solution (pH ~13.6) for 15 min to form a precipitate. The product was repeatedly rinsed with distilled water to lower the pH below 8 and remove excess precipitate. Although minor quantities of iron (hydr)oxide species may be present, Hristovski et al. [15] confirmed using X-ray diffraction that the dominant form of synthesized iron (hydr)oxide during both synthesis methods is amorphous FeOOH. The prepared materials were air-dried, crushed, sieved using US mesh 40 × 60, and stored wet prior to use in arsenic adsorption experiments.

2.2. Characterization of Fe-GAC

The iron contents of the Fe-GAC samples were determined by acid digestion in concentrated HNO_3 and 30% H_2O_2 (US EPA SWA 846, Method 3050B) followed by flame-atomic absorption spectroscopy (Varian Spectra 50B) [16]. Before the acid digestion, samples were ground to a powder and dried at 104 °C to constant mass to remove any moisture. The permanganate concentration was measured using a UV–vis spectrophotometer (Jenway 6405, Barloworld Scientific Ltd., UK) according to Analytical Method 102 [17].

The iron and manganese distributions throughout the Fe-GAC were evaluated by multipoint EDX microanalysis (EDAX Inc.) along a cross-section line. The carbon samples were glued to an epoxy resin and sliced to reveal the inner core of the particle. FIB and SEM techniques were employed to determine the size and shape of the deposited iron (hydr)oxide nanoparticles within the pores of the media (Nova 200 NanoLab UHR FEG-SEM/FIB and XL 30 by FEI). A backscatter detector was used to differentiate the iron from the carbon inside the Fe-GAC. This backscatter detector differentiated between heavier elements such as iron, which appear as whiter areas, and lighter elements such as carbon, nitrogen, oxygen and hydrogen, which appear as darker areas.

Arsenic was analyzed using a graphite furnace atomic absorption spectrophotometer (GF-AAS) Varian Zeeman Spectra 400 [18].

2.3. Equilibrium adsorption experiments

To study the impact of pH on the affinity of Fe-GAC for arsenic, batch adsorption experiments were conducted in 500 mL HDPE bottles (Nalgene). Fe-GAC samples (4–1250 mg/L Fe-GAC by dry weight) were mixed with solutions of 10 mM $NaHCO_3$-buffered ultrapure water containing 120 μg/L As(V) and having a pH range of 6.2 ± 0.1–10.0 ± 0.1. Samples were continuously agitated for 3 days prior to filtering through a 0.8-μm acetate membrane filter. Arsenate adsorption isotherms were plotted using the Freundlich adsorption isotherm model is given by the following equation:

$$q = KC_E^{1/n} \quad (2)$$

where q is adsorption capacity (μg adsorbate/g adsorbent), K is the Freundlich adsorption capacity parameter ((μg adsorbate/g adsorbent)(L/μg adsorbate)$^{1/n}$), C_E is the equilibrium concentration of adsorbate in solution (μg adsorbate/L), and $1/n$ is the Freundlich adsorption intensity parameter.

Table 2
Synthesis conditions and iron content of the Fe-GAC media synthesized via the $KMnO_4$/Fe(II) treatment method

Fe-GAC ID	MnO_4^- concentration	Contact time for MnO_4^- and GAC (min)	%Fe in dry Fe-GAC
Mn1	0.1N	15	10.7
Mn2	0.1N	45	10.2
Mn3	0.1N	120	10.3
Mn4	0.5N	15	16.4
Mn5	0.5N	45	15.7
Mn0	NA	180	2.8

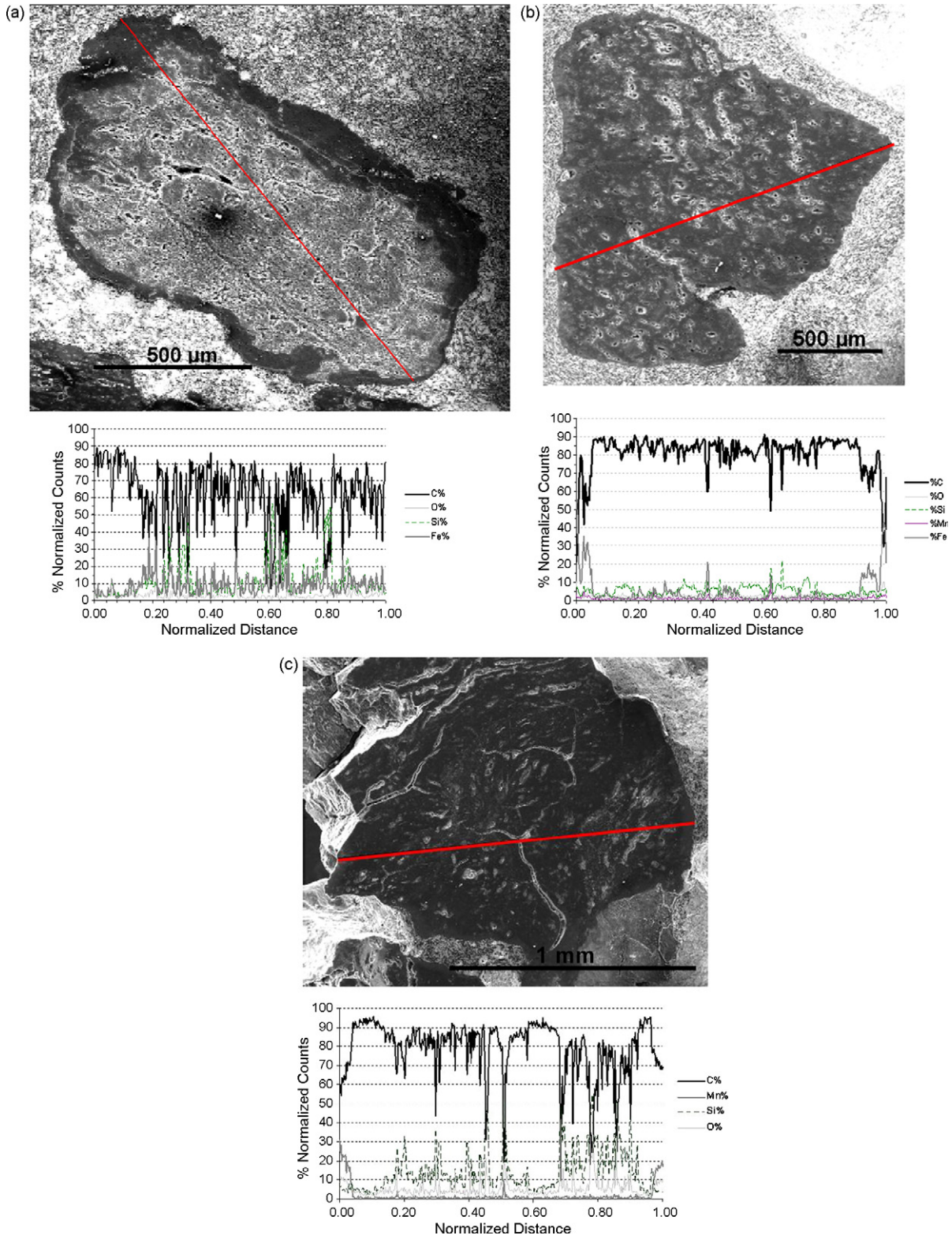

Fig. 1. (a) SEM image of a cross-section through a Fe-GAC particle synthesized via the Fe(III)/alcohol method and the particle's iron distribution, as analyzed with electron dispersion X-ray microanalysis (EDX). (b) SEM image of a cross-section through a Fe-GAC particle via a pre-oxidation step using $KMnO_4$ and the particle's iron distribution, as analyzed with electron dispersion X-ray (EDX) microanalysis. (c) SEM image of a cross-section through a GAC particle treated with $KMnO_4$ only for period of 45 min and the particle's manganese distribution, as analyzed with electron dispersion X-ray (EDX) microanalysis.

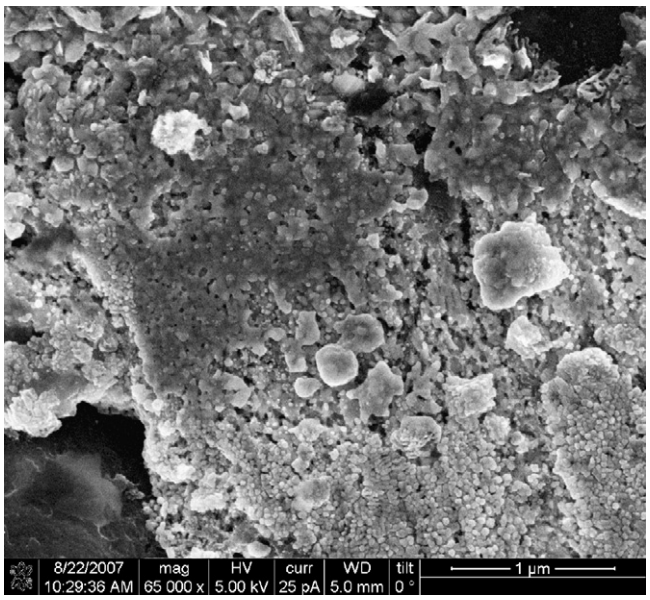

Fig. 2. Iron (hydr)oxide clusters formed in the large pores of Fe-GAC synthesized via the Fe(III)/alcohol method; the nanoparticles in the clusters are spherical.

3. Results and discussion

3.1. Impact of synthesis conditions on iron loading on Fe-GAC

The iron content of the untreated GAC was <0.05% of Fe per dry carbon weight. The iron content of the Fe-GAC prepared via the Fe(III)/alcohol method ranged from 0.5% to 12.5% Fe per dry carbon weight (Table 1). The iron loading on the carbon increased as the Fe(III) concentration in alcohol increased. The samples synthesized using 3N and 6N Fe^{3+} yielded 9% and 12% iron/g of dry Fe-GAC, respectively. Raising the iron concentration 10-fold from 0.03 to 0.3 M increased the iron loading in the Fe-GAC by four to six times. When the iron concentration was raised 200-fold, 25 times more iron was impregnated in the Fe-GAC.

Initially, longer contact times were expected to increase the iron content of the Fe-GAC by allowing more time for Fe^{3+} to diffuse deeper into the GAC particles and for a pseudo-equilibrium to be established between the iron concentration in the bulk solution and that in the carbon. However, the results suggest that contact time did not have a significant effect on iron loading. Fe-GAC synthesized with constant Fe(III) concentrations in alcohol but different contact times resulted in material with the same iron content. This indicated that a contact time of 15 min or even less may be sufficient to establish a pseudo-equilibrium, which may be an advantage when conducting a synthesis on a large scale. Additionally, prolonged contact times can contribute to increased attrition of the GAC material which could result in consequent loss of iron from the media. Although the iron content data presented in Table 1 does not exhibit scientifically significant variance, one can suggest a trend of small decrease in iron content with increase in contact time.

Higher iron contents were generally obtained using the $KMnO_4$/Fe(II) method; these Fe-GAC samples had 10–16% Fe per dry adsorbent weight (Table 2). The iron content of the Fe-GAC pretreated with permanganate increased as the permanganate concentration increased. The Fe-GAC obtained by contacting the carbon with only 1 M $FeSO_4 \cdot 7H_2O$ (no $KMnO_4$ pretreatment) had a very low iron content, 2.8% Fe per dry carbon weight. This demonstrates that the pre-oxidation step in this synthesis method is essential to obtain good iron loading. Pretreatment with 0.5N $KMnO_4$ yielded a product with ~160 mg Fe/g dry carbon.

3.2. Iron distribution in Fe-GAC

Fig. 1a presents a SEM image of a cross-section through a grain of Fe-GAC synthesized via the Fe(III)/alcohol method and the distribution of iron obtained via the EDX technique. Regions of high iron concentration correspond to the locations of large pores in the GAC. FIB/SEM analysis verified the presence of large iron nanoparticle clusters in these locations. These nanoparticles were spherical in shape with sizes ranging from 20 to 100 nm, which is generally consistent with the nanoparticles produced via the Fe(III)/alcohol method (Fig. 2).

The distribution of iron across the Fe-GAC particle cross-section was uneven when the $KMnO_4$/Fe(II) synthesis method was used (Fig. 1b). Most of the iron was concentrated near the outer edges of the media, with the exception of several peaks that correspond to iron located in larger pores. When a sample was treated only with a permanganate solution (no Fe(II) added), the manganese distribution was similar to that for the iron (Fig. 1c). This distribution pattern was seen in all Fe-GAC synthesized using the permanganate method. The surface active Mn-forms appear to focus the formation of FeOOH on the GAC surface.

The Fe-GAC synthesized via the $KMnO_4$/Fe(II) method contained iron nanoparticles that were about 30 nm long, 5 nm thick, and tooth-like in shape (Fig. 3). These particles did not resemble the spherical nanoparticles produced with the Fe(III)/alcohol method (Fig. 2). Interestingly, however, spherical iron oxide nanoparticles could be found in the inner parts of this Fe-GAC, i.e., in parts of the carbon where very little or no interaction between permanganate and the GAC surface had occurred. This suggests that the pre-oxidation step using permanganate may direct the shape of the iron oxide nanoparticles that form later in the synthesis.

3.3. Tracking manganese during synthesis

Manganese was tracked during synthesis to better understand its role in the formation and distribution of iron nanoparticles. During the pre-oxidation step with 0.1N $KMnO_4$, more than 92% of the permanganate was reduced within the first 15 min. In addi-

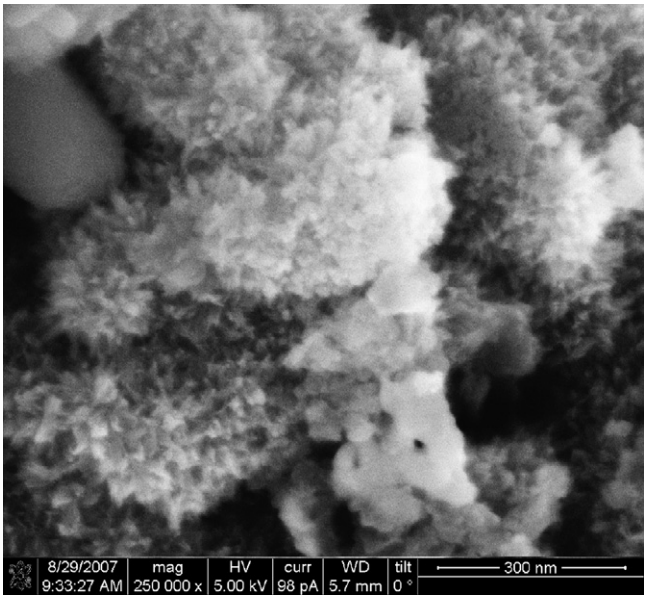

Fig. 3. The iron (hydr)oxide nanoparticles that formed in the outside layer of Fe-GAC obtained via $KMnO_4$/Fe(II) method are tooth-like in shape.

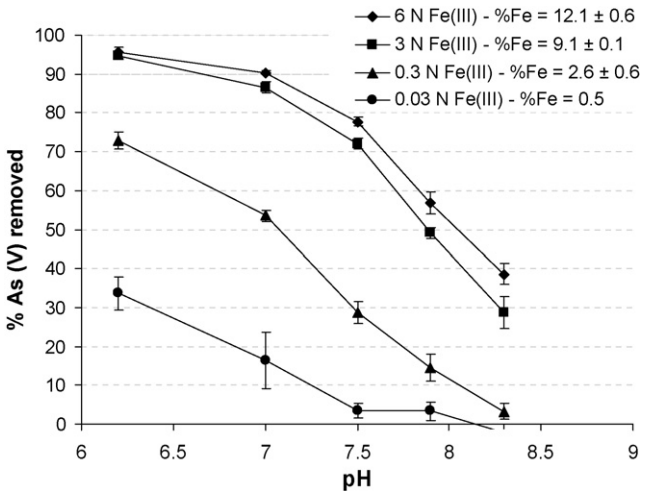

Fig. 4. The affinity for As(V) of Fe-GAC synthesized via the Fe(III)/alcohol method, as a function of pH. %As(V) removed by 1 g/L dry FE-GAC at different pH values; contact time = 3 days; 10 mM $NaHCO_3$; initial As(V) concentration ~120 μg L^{-1}.

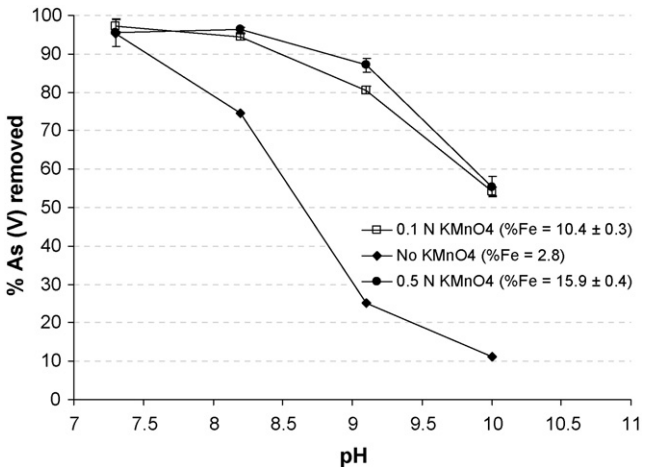

Fig. 5. The affinity for arsenic of Fe-GAC synthesized via the $KMnO_4$/Fe(II) method, as a function of pH. %As(V) removed by 1 g/L dry FE-GAC at different pH values; contact time = 3 days; 10 mM $NaHCO_3$; initial As(V) concentration ~120 μg L^{-1}.

tion, more than 70% of the total manganese remained inside the GAC after contact (Table 3). Furthermore, the amount of manganese remaining inside the GAC after the oxidation step increased as contact time increased. The maximum amount of manganese that remained inside the pores after a contact time of 120 min was 75%. In contrast, when a higher concentration of $KMnO_4$ (0.5N) was used, 32% and ~8% of the permanganate remained unreacted (in solution) after 15 and 45 min of contact time, respectively. Only 47–51% of the total manganese remained inside the GAC after the 15 and 45 min reaction times, indicating that $KMnO_4$ was present in high excess (Table 3).

Contacting the pre-oxidized GAC with Fe(II)SO_4 subsequently resulted in oxidation and precipitation of the iron but also in the release of the GAC-bound manganese. After this step, less than 0.2% of the initial manganese remained inside the GAC when 0.1N $KMnO_4$ was used, but more than 10 times that amount remained with 0.5N $KMnO_4$. The amount of Mn remaining was less than 5% when a long contact time was used (45 min).

The oxidation state of Mn may go through several transformations in the synthesis. Upon initial contact with the carbon, manganese (as $KMnO_4$) is partially reduced from Mn^{7+} to more stable manganese forms (e.g., Mn^{4+}). The partially reduced manganese is then deposited inside the pores of the GAC as insoluble manganese oxide (MnO_x). The addition of Fe(II) further reduces the MnO_x to Mn^{2+} as Fe^{2+} oxidizes to Fe^{3+}. Divalent manganese is soluble and the most stable form of manganese. The oxidized Fe(II) then precipitates as nanoparticulate FeOOH.

3.4. Affinity of Fe-GAC for arsenic

Fig. 4 shows the effect of pH on the arsenic removal efficiency of Fe-GAC prepared via the Fe(III)/alcohol method. Arsenate removal was highest for the samples with the highest iron contents, 90–120 mg Fe/g dry carbon (Fig. 4). Increasing the pH reduced the arsenic capacity of Fe-GAC, which is consistent with iron and arsenic chemistry well described in the literature [2,19,20].

Fe-GAC synthesized via the $KMnO_4$/Fe(II) method had a higher arsenate removal capacity at pH of 8.3 ± 0.1 than Fe-GAC obtained via the Fe(III)/alcohol method (each with 159 mg Fe/g dry carbon). The former removed almost 95% of the arsenate, while the latter at best removed 30–40% (Fig. 5). The pH had a weaker effect on Fe-GAC synthesized via the $KMnO_4$/Fe(II) method than on the Fe-GAC prepared via the Fe(III)/alcohol method, as Fe-GAC/$KMnO_4$ still removed more than 50% of the arsenate at pH 10 ± 0.1. These results suggest that arsenate removal capacity does not increase significantly when the iron content is more than 100 mg Fe/g dry carbon. This may be due to the formation of large iron (hydr)oxide particles that clog the pores, which causes available adsorption sites to be inaccessible to arsenic.

3.5. Arsenic(V) adsorption isotherms

Arsenic(V) adsorption isotherm experiments were conducted at two pH values (6.4 and 8.3) to further study the properties of Fe-GAC prepared using the two different synthesis methods. The pH values were selected because the pH of most natural waters is within this range.

Arsenate adsorption isotherms were plotted at the two pH values for four samples with different iron loadings (Fig. 6). At both pH values, Fe-GAC prepared via the permanganate method exhibited a considerably higher adsorption capacity than the media obtained via the Fe(III)/alcohol method; this was also evident in the single-dose experiments. As shown in Table 4, the adsorption capacity parameter (K) values for the media synthesized using the permanganate method were an order of magnitude higher than those for

Table 3
Mass balance of manganese in the KMnO4/Fe(II) method (Bold and italic values represent sums of the corresponding columns)

Fe-GAC	(*A*) %Mn as unreacted MnO_4 remaining in solution after Step 1	(*B*) %Mn as reduced form of Mn remaining in solution after Step 1	(*C*) Total %Mn remaining in solution after Step 1 (*C* = *A* + *B*)	(*D*) %Mn remaining in the GAC after Step 1 (*D* = *F* + *E*)	(*E*) %Mn released into solution after Step 2	(*F*) %Mn still remaining in the GAC after Step 2	Total %Mn recovered (*G* = *A* + *B* + *D*)
Mn1	7.66	16.72	**24.38**	**70.53**	70.39	0.14	*94.91*
Mn2	0.00	18.71	**18.71**	**75.31**	75.18	0.13	*94.02*
Mn3	0.00	13.96	**13.96**	**75.32**	75.18	0.14	*89.28*
Mn4	32.41	20.38	**52.79**	**47.20**	46.10	1.10	*99.99*
Mn5	8.29	36.07	**44.36**	**51.18**	46.51	4.67	*95.54*

Table 4
Fitted adsorption capacity parameters (K) and Freundlich adsorption intensity parameters ($1/n$)[a]

Fe-GAC (%Fe)	pH 6.4 ± 0.1				pH 8.3 ± 0.1			
	K[b]	K[c]	$1/n$	R^2	K[b]	K[c]	$1/n$	R^2
Mn1 (10.7)	263.6	2,643.1	0.41	0.99	31.5	294.4	0.62	0.99
Mn4 (16.4)	247.2	2,310,1	0.48	0.98	47.3	442.0	0.58	0.97
M7 (9.1)	37.9	354,2	0.49	0.95	0.0002	0.002	2.63	0.98
M10 (12.4)	48.9	457,0	0.55	0.97	0.05	0.47	1.7	0.97

[a] Contact time = 3 days; 10 mM $NaHCO_3$-buffered ultrapure water; initial As(V) concentration ~120 μg/L.
[b] μgAs/g dry M-GAC/(μgAs/L)$^{1/n}$.
[c] μgAs/gFe/(μgAs/L)$^{1/n}$.

the samples prepared via the Fe(III)/alcohol method (~250 vs. ~45 at pH 6.4). A study conducted by Chen et al. [21] reported similar K values (K ~ 200 (μgAs(V)/g dry media) (L/μg)$^{1/n}$) for iron impregnated bituminous GAC at pH 6. However, these values are still several times lower than the K values (K ~ 4452 and ~429 (μgAs(V)/g dry media) (L/μg)$^{1/n}$)) reported for commercially available arsenic removal media such as granulated ferric hydroxide (GFH) [22,23]. Considering that iron content of GFH is in the range of approximately 50% in comparison to maximum of 15% for the Fe-GAC, one can attribute this higher adsorption capacity of GFH to the higher iron content. However, the advantage of the synthesized Fe-GAC is its potential ability to simultaneously remove arsenate and organic contaminants, whereas commercially available iron (hydr)oxides can only remove arsenate.

The Freundlich intensity parameters ($1/n$) for all Fe-GAC samples were <0.62 at pH 6.4 ± 0.1, suggesting favorable adsorption. The $1/n$ values for Fe-GAC/$KMnO_4$ remained relatively constant at pH 8.3, but the $1/n$ values increased significantly for the Fe-GAC obtained via the Fe(III)/alcohol method. The increased from ~0.5 to 1.7 and 2.6 for M7 and M10, respectively. Such large $1/n$ values suggest very unfavorable adsorption. This may be due to the electrostatic repulsion between the prevalent $HAsO_4^{2-}$ species and the negatively charged Fe–carbon surface, which should be dominant at high pH.

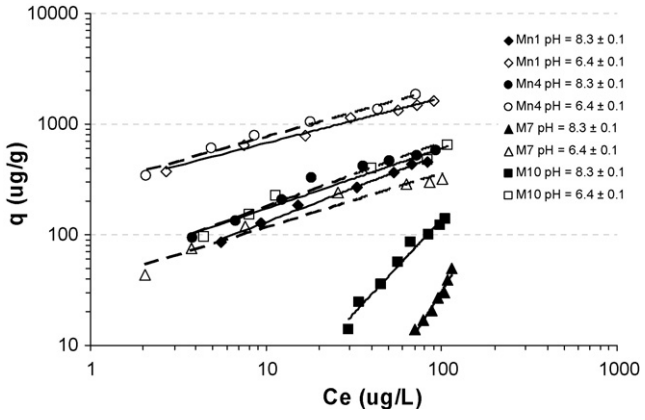

Fig. 6. Arsenate adsorption isotherms for Fe-GAC samples with various iron contents, prepared using the two different synthesis methods in 10 mM $NaHCO_3$-buffered ultrapure water and with a contact time of 3 days (initial As(V) concentration ~120 μg L^{-1}).

4. Conclusion

During the development of GAC impregnated with iron (hydr)oxide nanoparticles for arsenate treatment, two different preparative methods were used to study the effect of synthesis conditions on the formation of the iron oxide nanoparticles in the GAC and on the material's arsenic adsorption capacity. In general, the arsenic removal capacity of Fe-GAC increased as the iron content of the Fe-GAC increased. However, the iron content did not significantly increase at iron solution concentrations higher than 3N and 6N when the Fe(III)/alcohol synthesis method was used. Furthermore, a synthesis contact time longer than 15 min did not seem to have a significant effect on the iron content of the Fe-GAC.

The use of an oxidant ($KMnO_4$) affected the distribution and shape of the iron (hydr)oxide nanoparticles. While the absence of permanganate pretreatment yielded spherical nanoparticles distributed throughout the Fe-GAC media, the introduction of permanganate yielded teeth-like nanoparticles that were generally distributed in the outer layer of the media, i.e., where permanganate and GAC had interacted. The data obtained from manganese mass balance calculations suggest that permanganate is partially reduced and precipitated on the GAC surface during the first step of the process, and then it is further reduced to soluble divalent manganese during the step in which Fe(II) is oxidized and iron (hydr)oxide formed. Fe-GAC produced via the permanganate/Fe(II) method had an order of magnitude greater As(V) capacity than the sample obtained using direct precipitation of Fe(III). To develop media with improved arsenate adsorption properties, it is essential to better understand the factors that control metal (hydr)oxide nanoparticle formation onto specific supporting surfaces, such as GAC.

References

[1] US Department of Health and Human Services (Ed.), Toxicological Profile for Arsenic, US Department of Health and Human Services, Washington, DC, 2000.
[2] P.L. Smedley, D.G. Kinniburgh, A review of the source, behaviour and distribution of arsenic in natural waters, Appl. Geochem. 17 (5) (2002) 517–568.
[3] R.D. Foust, P. Mohapatra, A.M. Compton-O'Brien, J. Reifel, Groundwater arsenic in the Verde valley in central Arizona, USA, Appl. Geochem. 19 (2) (2004) 251–255.
[4] R.J. Edmonds, D.J. Gellenbeck, Ground water quality in the west Salt River Valley, Arizona 1996–98—relations to hydrogeology, water use, and land use, Tucson, Arizona, USGS No. 01-4126, 2002.
[5] US EPA, Implementation Guidance for the Arsenic Rule, Office of Water, US EPA, Washington, DC, 2002, EPA-816-K-02-018.
[6] EU Council. Council Directive 98/83/EC of 3 November 1998 on the quality of water intended for human consumption, Off. J. Eur. Commun. L 330 (1998) 32–54.
[7] WHO (Ed.), Guidelines for Drinking-Water Quality, 3rd ed., World Health Organization, Geneva, 2004.
[8] R.P.S. Suri, J.B. Liu, J.C. Crittenden, D.W. Hand, Removal and destruction of organic contaminants in water using adsorption, steam regeneration, and photocatalytic oxidation. A pilot-scale study, J Air Waste Manage. Assoc. 49 (8) (1999) 951–958.
[9] Z.M. Gu, J. Fang, B.L. Deng, Preparation and evaluation of GAC-based iron-containing adsorbents for arsenic removal, Environ. Sci. Technol. 39 (10) (2005) 3833–3843.
[10] M.J. DeMarco, A.K. Sengupta, J.E. Greenleaf, Arsenic removal using a polymeric/inorganic hybrid sorbent, Water Res. 37 (1) (2003) 164–176.
[11] A.I. Zouboulis, I.A. Katsoyiannis, Arsenic removal using iron oxide loaded alginate beads, Ind. Eng. Chem. Res. 41 (24) (2002) 6149–6155.
[12] F.S. Zhang, H. Itoh, Iron oxide-loaded slag for arsenic removal from aqueous system, Chemosphere 60 (3) (2005) 319–325.
[13] M.C. Lee, V.L. Snoeyink, J.C. Crittenden, Activated carbon adsorption of humic substances, J. AWWA 73 (8) (1981) 440–460.
[14] A.K. Sengupta, L.H. Cumbal, Method of manufacture and use of hybrid anion exchanger for selective removal of contaminating fluids, US Patent Application 20,050,156,136 (July 21, 2005).
[15] K. Hristovski, P. Westerhoff, T. Möller, P. Sylvester, W. Condit, H. Mash, Simultaneous removal of perchlorate and arsenate by ion-exchange media modified with nanostructured iron (hydr)oxide, J. Hazard. Mater. 152 (1) (2008) 397–406.
[16] US EPA. SW-846 test methods for evaluating solid waste, Physical/Chemical methods, US EPA, Washington, DC, USA, 1996.

[17] Carus Chemical Company, Analytical Method 102: Determination of Potassium Permanganate Residual for Drinking Water Treatment, Carus Chemical Company, Peru, IL, USA, 2004.
[18] M.A.H. Franson, A.D. Eaton, L.S. Clesceri, A.E. Greenberg (Eds.), Standard Methods for the Examination of Water and Wastewater, 19th ed., American Public Health Association, Washington DC, USA, 1995.
[19] P.K. Dutta, A.K. Ray, V.K. Sharma, F.J. Millero, Adsorption of arsenate and arsenite on titanium dioxide suspensions, J. Colloid Interf. Sci. 278 (2) (2004) 270–275.
[20] M. Badruzzaman, Mass transport scaling and the role of silica on arsenic adsorption onto porous iron oxide (hydroxide), Arizona State University Ph.D. Dissertation, Tempe, AZ, USA, 2005.
[21] W. Chen, R. Parette, J. Zou, F.S. Cannon, B.A. Dempsey, Arsenic removal by iron-modified activated carbon, Water Res. 41 (9) (2007) 1851–1858.
[22] M. Badruzzaman, P. Westerhoff, D.R.U. Knappe, Intraparticle diffusion and adsorption of arsenate onto granular ferric hydroxide (GFH), Water Res. 38 (18) (2004) 4002–4012.
[23] A. Sperlich, A. Werner, A. Genz, G. Amy, E. Worch, M. Jekel, Breakthrough behavior of granular ferric hydroxide (GFH) fixed-bed adsorption filters. Modeling and experimental approaches, Water Res. 39 (6) (2005) 1190–1198.